Journal of Thermal Analysis and Calorimetry, Vol. 59 (2000) 205–225

Dedicated to Prof. Edith A. Turi in recognition of her leadership in education

GLASS AND STRUCTURAL TRANSITIONS MEASURED AT POLYMER SURFACES ON THE NANOSCALE

R. M. Overney[1], *C. Buenviaje*[1], *R. Luginbühl*[2] *and F. Dinelli*[1]

[1]Department of Chemical Engineering, University of Washington, Box 351750, Seattle WA 98195-1750
[2]University of Washington Engineered Biomaterials and Department of Bioengineering University of Washington, Box 351750, Seattle, WA 98195-1750 USA

Abstract

This paper reviews our recent progress in determining the surface glass transition temperature, T_g, of free and substrate confined amorphous polymer films. We will introduce novel instrumental approaches and discuss surface and bulk concepts of T_g. The T_g of surfaces will be compared to the bulk, and we will discuss the effect of interfacial interactions (confinements), surface energy, disentanglement, adhesion forces, viscosity and structural changes on the glass transition. Measurements have been conducted with scanning force microscopy in two different shear modes: dynamic friction force mode and locally static shear modulation mode. The applicability of these two nano-contact modes to T_g will be discussed.

Keywords: atomic force microscopy (AFM), confinement, friction, glass transition, polymers, scanning force microscopy (SFM), scanning probe microscopy (SPM), shear modulation, surface analysis, surface interaction

Introduction

The glass transition temperature, T_g, of amorphous polymers is recognized as one of the most important parameters for technological applications. At temperatures above T_g, a noncrystalline polymer material behaves rubbery, or like a viscous fluid, depending on the molecular weight and how much the temperature exceeds the glass transition temperature. Below T_g, a bulk polymer is described as a glass that is more or less brittle (remaining flexibility might be provided by side-chains) depending on the structural complexity and how much it is cooled down.

Any influence on the glass transition due to interfacial interactions is usually neglected even for films thinner than the bulk radius of gyration. The major reason for such 'free' boundary conditions originates from classical mean-field theories, or molecular dynamic simulations. It is assumed that interfacial interactions are completely screened within a distance corresponding to the persistence length of the polymer [1, 2]. Thus, confinement effects due to interfacial interactions, such as pinning of molecules at substrate surfaces, are only considered up to 0.6 to 1 nm distance [2]. Not considered in such scaling theories are effects that occur during the film coating pro-

1418–2874/2000/ $ 5.00
Akadémiai Kiadó, Budapest
© 2000 Akadémiai Kiadó, Budapest
Kluwer Academic Publishers, Dordrecht

cess, for instance, fast solvent evaporation. These effects may be very important in polymer coating procedures which are highly relevant for many technological applications, such as spin casting [3, 4]. We have found, for instance, that interfacial interactions can affect the polymer film up to a distance of 200 nm from the substrate interface, even after temperature annealing [3, 5, 6].

Two interfaces have to be considered for thin films: (i) the interface with the substrate, and (ii) the air (or liquid-) polymer interface (*free surface*). Recent results from several groups suggest an unchanged or increased molecular mobility at the free surface of thick films [7, 8]. A reduced molecular mobility at the surface of ultrathin films was reported based on forward recoil spectroscopy measurements [9], fluorescence recovery after patterned photobleaching (FRAPP) [10], and scanning force microscopy (SFM) [3, 6]. No evidence was found that the surface T_g is different from the bulk T_g for polystyrene (PS) films with a high molecular weight on the order of 2×10^4 [7]. A strong reduction in the surface T_g was, however, found for lower molecular weight PS films [7].

It is reasonable to assume that in a confined polymer system the glass transition temperature is altered. Novel techniques such as near-edge X-ray absorption fine structure (NEXAFS) spectroscopy [8], X-rays diffraction [10–13], slow-positron-annihilation spectroscopy (SPAP) [14, 15], Brillouin light scattering (BLS) [16], spectroscopic ellipsometry (SE) [17], attenuated total reflection (ATR) [18], and scanning force microscopy (SFM) [19–22] have been employed to determine T_g for ultrathin polymer films or transitions that are associated with the rotational freedom of side-groups [22]. Although these techniques have been applied to similar systems (monodisperse polystyrene films, $M_w>30k$, spin cast on silicon), conclusions are quite controversial. Authors using the SPAP, BLS, SE and ATR techniques predict a decrease in T_g closer to the solid substrate, while results obtained by NEXAFS, X-rays diffraction and SFM [19, 20] suggest that T_g increases in the vicinity of a confining interface. Jean *et al.* assume that polymer molecules near the solid surface are incomplete or partially entangled. Based on that assumption, they claim that T_g has to decrease close to the solid surface [14]. On a similar system, we observed experimentally that indeed the molecules are disentangled at the silicon surface due to the spin casting process [6]. At a thickness of about 20 nm (which is comparable to the radius of gyration, R_g, of the polymer) a gel-like substructure with a significantly decreased density was found. The substructure, as we will discuss in detail below, does not anneal even at temperatures far above T_g. Most of the techniques listed above are sensitive to the free-volume and this information is used to make predictions about the glass transition. Thus, existing static heterogeneities (different from dynamic heterogeneities [23]) in spin cast films could explain part of the controversy. The free-volume theory (discussed below) postulates that the segmental volume changes at T_g. However, it does not postulate the reverse statement, i.e., that in the event of a free-volume change, the polymer has unconditionally to go through a glass transition.

If a new technique is added to others that are well established, it is important to re-investigate the physical principles that determine the quantity of interest. This involves gaining a certain understanding of the classical theories, i.e., to familiarize

oneself with the commonly used terminology and definitions. Hence, we review very briefly conceptual ideas and observations concerning the glass transition temperature (next paragraph) before discussing our observations obtained by SFM on the nanoscale.

The glass transition temperature of amorphous bulk polymers

Illustratively, the rubbery state of an amorphous polymer may be regarded as the situation in which entanglements are restricting the motion of complete chains with respect to each other. Only the coiled sections of the chains lying between entanglements are moving and provide the polymer with a rubbery characteristic. At higher temperatures, i.e., at temperatures at which entanglements are substantially resolved, the polymer will behave like a viscous fluid and respond to stress by plastic flow. Hence, to minimize or avoid permanent plastic damage when stress is applied, for instance, synthetic rubbers are specially treated to increase the cross-linking density. As the temperature is lowered below the glass transition temperature, the amorphous polymer changes in many of its properties. For instance, mechanical properties such as elastic moduli and damping change significantly. The material complies within a certain stress limit without plastic deformation. Exceeding this critical stress, the material will break rather than plastically deform. Hence, the glass transition temperature may be regarded in a very simplistic way as a critical temperature above which the polymer chains can partially move (*local segmental motion*), and below which the intermediate length scale of partial freedom of motion or diffusion is *frozen*. Other material properties, which are affected by the glass transition temperature, are the specific volume and heat, the refractive index and dielectric loss. The refractive index and the dielectric loss are increasingly important in mechanical contact measurements and will be discussed in more detail below.

Quite extensive literature that deals with the determination and the interpretation of the glass transition temperature can be found starting from simple linear chained amorphous polymers to complex graft-copolymers and polymers with partially crystalline structure [24]. For instance, it was found that polymers show many characteristics of a second-order phase transition in which a primary thermodynamic function, such as the volume or heat content, change in slope with temperature at T_g. This brings up one of the major controversies about the glass transition temperature. Is the T_g a purely kinetic phenomenon, i.e., a non-equilibrium conformation, or does T_g exist whether or not the polymer is in equilibrium; i.e., is T_g a second-order phase transition? Although there is up-to-date no conclusive evidence available to confirm either of these ideas, very useful theories have been developed favoring the non-equilibrium conformation of polymers at T_g [25–27]. The non-equilibrium conformation describes T_g as the temperature at which segmental motion in the chains becomes so slow that equilibrium conditions cannot be maintained and the material is confined or frozen. This idea is experimentally supported by the cooling rate dependence of T_g. Quite successful kinetic theories have been developed in the 1950's. One of them

considers T_g as an iso-elastic temperature [26] while another considers T_g as an iso-free volume property [25, 27]. The iso-free volume theory has been found to be a simplifying form of the iso-elastic theory if one assumes that the free-volume is generated by rotational motions of the backbone segments [28].

The free volume theory is based on the exponential relationship between the viscosity η and the ratio of the occupied and free volume, V_0 and V_f, respectively, i.e,

$$\eta = A\exp\left(B\frac{V_0}{V_f}\right) \tag{1}$$

with the constants A and B [29]. Introducing the free volume fraction f and f_g at the temperature T and T_g, respectively, where the volume fraction is defined as

$$f = \frac{V_f}{V_0 + V_f} \tag{2}$$

the Williams-Landell-Ferry (WLF) equation can be derived [27]. In approximated form the WLF equation is [27]:

$$\frac{1}{2.3}\ln\left(\frac{\eta_T}{\eta_{T_g}}\right) = \frac{1}{2.3}\ln(a_T) \approx -\frac{1}{2.3 f_g}\left(\frac{T - T_g}{(f_g/\alpha_f) + T - T_g}\right) = -17.4\left(\frac{T - T_g}{51.6 + T - T_g}\right) \tag{3}$$

where the ratio of the viscosity at T and T_g is a shift factor, a_T, which can be expressed as a function of the difference between the glass transition and the actual temperature, and the ratio of the free volume at the glass transition and the expansion coefficient above the glass transition α_f. The constants 17.4 and 51.6 are found to be valid for a wide range of materials.

Complex thermodynamic theories based on the Gibbs-Di Mario theory have been employed to determine configurational entropy as a function of the glass transition temperature [30]. Based on these theories, a thermodynamic glass transition exists which is close to the one observed kinetically. However, under normal kinetic conditions, equilibrium cannot be reached but only approached with decreasing cooling rates. The thermodynamic approach has been found to be very fruitful and is in good agreement with experiments where T_g has been studied, for instance, as a function of cross-linking density, plasticizer content and molecular weight [24, 30]. In recent theoretical work, the equilibrium theories for T_g are still heavily disputed and true equilibrium is found to exist only for systems of infinite molecular weight with conventional intermolecular interactions [31].

There are many degrees of freedom that affect the glass transition. Experiments are heavily focusing on the effect of the molecular structure [24, 28]. It was, for instance, found that the single chain influences T_g through its stiffness and tacticity. Interactions between chains such as cohesive energy density, dipole attraction, H-bonding also modify T_g. Other structural effects, which alter T_g, are molecular symmetry, copolymerization, molecular weight, branching and cross-linking. Be-

sides T_g that is associated with the onset of motion in the backbone of polymer chains, more transitions have been found at lower temperatures. These transitions are associated with the rotational freedom of side-groups.

It is the degree of freedom and its effect on the glass transition temperature that is placed in the center of discussion in this review. We will discuss the effect of interfacial confinement on changes in the glass transition temperature due to structural inhomogeneities. Further, we will critically evaluate the novel method we employed and discuss the material properties, which it is sensitive to.

Materials and instrumentation

Substrate and sample preparation

All organic solvents were of HPLC grade (Aldrich), except for ethanol (dehydrated, 200 Proof McCormick), and were used without further purification. Silicon wafers (100, Silicon Sense Inc, Santa Clara, CA) diced into 1 cm^2 pieces were cleaned in isopropanol and methylene chloride. The silicon substrates were hydrogen passivated by etching with aqueous hydrofluoric acid (40%, Fisher) for 5 minutes. Subsequently the substrates were rinsed with nanopure water (>18 MΩ) and dried in a stream of nitrogen. Some silicon substrates were coated with octadecyltrichlorosilane (OTS) or polyvinyl pyridine (PVP) to produce a low interaction interface prior to depositing thin polymer films. The OTS films were produced by dip coating from a dilute hexadecane/CCl_4/CH_3Cl solution. The PVP films were spin coated from toluene.

Poly(*t*-butyl)acrylate (PtBA, MW 138 kD, Polymer Source), and polystyrene (PS, MW 90 kD, Aldrich) were dissolved in toluene. A 250 µl polymer solution was applied onto the samples and a film spin coated at room temperature and 2500 rpm for 1 minute. The polymer film thickness was estimated from ellipsometry measurements. Changing the concentration of the diluted solution, the thickness of the polymer film was varied. After spin coating the samples were annealed in vacuum ($<10^{-5}$ bar) for 24 h at 160°C (PtBA) and 170°C (PS) and quenched by fast cooling to room temperature.

N-isopropylacrylamide (NIPAM) deposition was carried out by radio frequency plasma enhanced chemical vapor deposition (RF-PECVD, plasma deposition) in a reactor tube equipped with symmetrical external, capacitively coupled electrodes. The plasma was induced by a radio frequency of 13.56 MHz and maintained via matching network. Exact reaction conditions and a detailed description of the plasma reactor have been published elsewhere [32–35].

Scanning force microscopy

All measurements were performed on a commercial Explorer standalone system (ThermoMicroscopes) equipped with a standard 100 µm X-Y scanner and a 10 µm Z-piezo. The SFM system is based on an optical lever detection scheme and was used in conjunction with a digital oscilloscope using a very stable low frequency

(1–20 Hz) trigger system for lateral force (friction) measurements, and a dual-phase lock-in amplifier and a function generator for force modulation measurements. Experiments were carried out in a well-controlled environment at ambient temperature and pressure. T_g measurements on polymers were typically performed in a nitrogen-flooded dry box (humidity <4 % at 22°C), while NIPAM experiments were conducted using an open 2 ml liquid cell. Various bar shaped silicon and silicon nitride cantilevers were used with resonance frequencies between 9 and 100 kHz (NT-MDT, Russia and Nanosensors GmbH, Germany).

To quantify the results, SFM lateral force measurements were compared to a calibration standard [36]. The standard, i.e., a bar-shaped silicon cantilever and a silicon sample (cleaning method described elsewhere [36]) provides a calibration friction coefficient of μ_{cal} =0.18 ±0.02. It had been obtained by 20 μm scans at 20 μm s^{-1} under positive applied loads. The dimensions of the standard bar-shaped cantilever were determined by SEM and the normal and torsional spring constants, k_N and k_T, were calculated by

$$k_N = \frac{EWT^3}{4L^3} \tag{4}$$

$$k_T = \frac{GWT^3}{3LR^2} \tag{5}$$

where E is the Young's modulus, G is the shear modulus [36], and W, T, L are the width, thickness and length respectively. Subsequent cantilevers, with known normal spring constants, were calibrated with the standard regarding the lateral force, F_L. The following relationship was employed:

$$F_L = \Gamma I_T;\ \Gamma = \mu_{cal}\left(\frac{\Delta I_T}{\Delta F_N}\right)^{-1}\Bigg|_{Si} \tag{6}$$

where F_N is the applied load, I_T is the torsional detection signal (in mV or nA) obtained for a 20 μm scan taken at 20 μm s^{-1} over the standard silicon (Si) surface, and Γ is the resulting geometrical calibration factor. (Example: The calibration geometry factor, Γ, was determined to be 5.3 for a 200 μm long triangular-shaped Si_3N_4 cantilever with k_N=0.064 N/m.)

Elastic and shear moduli were measured by distance modulation experiments either in normal or lateral direction. A sinusoidal signal (1–15 kHz) was added to the piezo signal input. The response to the sinusoidal stimulation was measured by a dual-phase lock-in amplifier (Stanford Research Systems) which provided amplitude, Δx_L, and phase, φ, components. Changes in the amplitude and phase were simultaneously recorded as a function of temperature using home-developed control and data acquisition software based on Labview (National Instruments).

Temperature stage

Major requirements for temperature control devices used in SFM are:

- small layouts to fit into the limited free space provided by many SFMs
- an adequate heating/cooling capacity (i.e., minimize transport due to radiation/convection, achieve thermal-equilibrium), and
- a fast response time to reach thermal-equilibrium within the time scale of the measurement.

Thermoelectric devices offer the requirement of being compact with a reasonably fast response time. Cooling is however a problem because of the small conduction/convection area. With increased contact area for efficient cooling, heat transfer by radiation and convection to the microscope cause thermal drifts and a non-equilibrium situation. In addition, single thermoelectric devices that are used for heating and cooling need a costly power supply, which reverses the polarity. A solution to these problems is to use two thermoelectric devices, a large one for cooling and a small one for heating. The drawback with that solution is a discontinuous operation around the environmental temperature.

In our experimental setup, we use a cooling device that is based on the rapid gas expansion from capillaries and uses an integrated thermoelectric device for heating. The stage was developed by MMR Technologies, Mountain View, CA (Model R2700-2) for high vacuum applications and was successfully tested in our laboratory within a temperature range of 220–425 K in a dry nitrogen environment at room temperature. The stage consists of a 15×8 mm^2 sample area at the end of a ceramic girder. SFM operational tests on ultra-flat samples, such as epitaxially grown calcium fluoride, indicated that there is no additional vibrational noise generated by the MMR device for nanometer-scale resolution imaging. This compact setup facilitates fast heating and cooling as the thermal insulation is optimized. The cooling is based on the Joule-Thompson effect and requires high-pressure nitrogen or argon gas. With the MMR device, we obtain fast responses (about 0.1–1°C s^{-1}) and very accurate temperature-control (0.05–0.1°C). We have found that this type of heating/cooling device is far superior to other systems tested.

Surface glass transition temperatures

Originally, two fundamental questions were driving this research:

a. Are polymer surfaces of amorphous bulk polymers constrained (frustrated) at the air-polymer interface for reasonably large molecular weight (>30*k*)?
b. Do solid interactive-interfaces confine the polymer matrix, and over what distance?

Both questions address possible changes in material properties, such as the glass transition temperature, and define interfacial boundary regions that are different from the bulk. A third, more instrumental question came up in the course of our experiments. What are nano-contact measurements sensitive to? The glass transition affects

many properties of the material as it was reviewed above. Are nano-contact measurements purely mechanical measurements, and thus mainly sensitive to changes in shear and elastic properties? Or, do also other properties, such as the refractive index and the dielectric loss affect the measurements?

Surface T_g of relatively thick films

A 'thick' film is defined as a film that does not reveal any property changes at the free-surface due to presence of the solid substrate. In the course of this paper, we will find that free-standing films (i.e., films with no solid substrate at either side) also belong to the class of films discussed here. In our first attempt to measure the glass transition temperature, we used a line-scan approach, i.e., we recorded lateral forces that were acting on our cantilever during the forward and reverse scan motion [37, 38]. From lateral force-loops, we determined the force difference that corresponds by a factor of two to the friction force [37]. Friction forces were recorded as function of the temperature by scanning the cantilever across the surface of thick films of poly(*t*-butyl) acrylate (PtBA) at a constant rate of 0.5 Hz over a distance of 20 μm, Fig. 1 [20]. A force-temperature transition was found at 304.8 K, as illustrated in Fig. 1. DSC measurements revealed that the glass transition temperature of PtBA is at 304 K, which is in good correspondence with our friction measurement. This is an interesting finding: *The surface T_g of an amorphous polymer is not different from the bulk.* We will provide below more evidence that will strengthen this statement as long as probing interferences, substrate interfacial effects or effects caused by the film preparation technique can be neglected.

Major probing interferences in thermally controlled SFM experiments are the applied load, the scan velocity, and the heating rate. It was reported by Somorjai and co-workers that glass transition measurements obtained by SFM-friction measurements are slightly higher than the ones determined by sum frequency generation and DSC [39]. The authors suggested that the applied load is responsible. In very recent

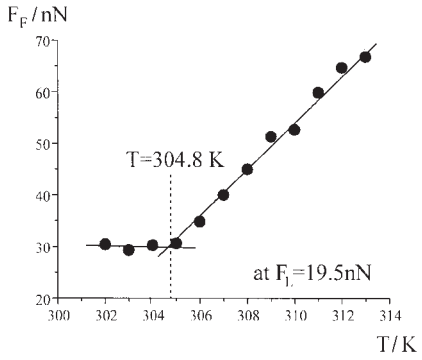

Fig. 1 Friction (F_F) *vs*. temperature (*T)* measured on a 160 nm thick PtBA film on silicon. The transition temperature corresponds to literature values measured by DSC

experiments, we found the statement of Somorjai confirmed, representing however an instrumental artifact [40]. It does not describe a property change in the polymer but an instrumental kinematic effect. The true transition value can be found by adjusting the load and the scan speed [40].

A fine terminological distinction has to be made between *applied load* and *normal force*. The normal force can be defined as the sum of the applied load plus the adhesive force. Hence, we can introduce an 'adhesion load' which corresponds to the normal force at a zero-bent cantilever in contact. This definition is important considering that the measurements can be conducted with different SFM tips. For instance, let us assume to have two chemically different functionalized cantilever tips. If brought into contact with the same homogeneous sample, they should show two distinct adhesion loads. We can assume that differences in the adhesive load would lead to differences in the recorded transitions, i.e., adhesion dependent effective glass transition temperatures. Hence, the probing material used for surface T_g measurement adds another possible probing interference. As a reminder, all the measurements reported in this paper were obtained with a probing tip of a native silicon oxide.

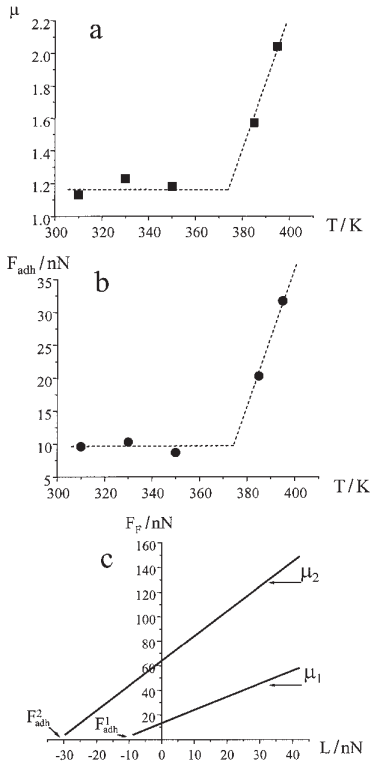

Fig. 2 Friction coefficient (μ) *vs*. temperature – a measure of γ (a). Adhesion (F_{adh}) *vs*. temperature – a measure of the contact area (b). Graphical representation of the cross-relationship between friction, adhesion and the coefficient of friction (determined from point 1 and 2 of Figs 2a and 2b) (c)

The friction force signal is affected by the contact area, the interfacial energy, γ, and the elastic modulus, E. Figure 2 shows details on how friction is changing as a function of the temperature measured on a thick PS film. As in the case of PtBA, we found a transition in the absolute friction force at the bulk T_g of 374 K, documented by the temperature plots of the friction coefficient, μ, and the adhesive force, F_{adh}, (Figs 2a, b). In Fig. 2c, the correlation between the adhesion force, the friction coefficient, and the friction force is illustrated by choosing two points from Fig. 2a and 2b. The friction force, F_F, is approximately described by Amontons law and an adhesive term, F_{adh}, i.e.,

$$F_F = \mu\,(L - F_{adh}) \tag{7}$$

where L represents the applied load, and μ the coefficient of friction. The adhesion force is by definition the force necessary to separate two surfaces in contact. Hence, F_{adh}, i.e, the intercept in Fig. 2c with the load axis, is strongly dependent on the contact area. A change in the contact area will not affect the slope of the curve but the intercept. The slope (i.e., the friction coefficient) is determined by the interfacial interaction strength, γ, and the elastic moduli of the sample, assuming a perfect contact of a uniform single asperity. Thus, Figs 2a and 2b are describing an increase in the interfacial interaction strength, the elastic moduli and the contact area, respectively, above the glass transition temperature. This result will be important for our interpretation of the shear modulation approach discussed below.

Measurements of ultrathin substrate confined films will be discussed later in detail. But there is one aspect, which is important in this discussion of the friction signal. Thin confined PS films showed qualitatively a similar trend of the friction force as illustrated in Figs 2a and 2c for thick PS films. The adhesion force, however, remained constant during the entire measurement. This indicated that changes in γ are very significant in SFM contact mechanical T_g measurements.

A novel approach to determine T_g – the surface shear modulation method

High yield stresses at the turning points during repeated forward and backward scanning motions of SFM friction measurements make the analysis quite cumbersome. Wear easily occurs in the static friction regime (called *stiction*) where the lateral traction reaches its maximum. The tip is easily soiled during that process which results in an increased contact area. This abrasive wear phenomenon is well known and addressed by various means [41].

The solution to stiction seems simple by avoiding turning points. This is however difficult to achieve during a scanning process, except one would scan on a closed and steady loop like on a spiral line. By modulating the cantilever in lateral direction, we found the perfect solution to avoid (or reduce) stiction problems at the turning points [19]. The principle is based on a small amplitude disturbance that is applied as a sinusoidal function in lateral direction while the tip is in contact with the sample at a constant load. If the lever shear-amplitude is chosen below the start-to-sliding resistance (set by the static friction value between tip and sample), the cantilever will only

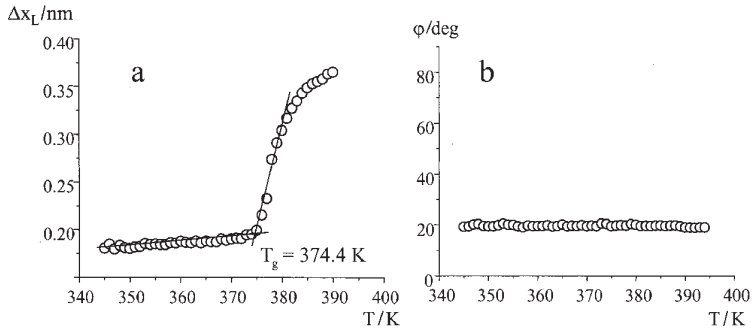

Fig. 3 Local no-slip shear modulation measurements *vs*. temperature. a) The sharp transition in the shear modulation response amplitude (Δx_L) corresponds to the glass transition temperature of 374 K. b) The phase shift between the input modulation and the response is about 11 degrees

deform the sample but it will not slide. The deformation of the sample, Δx_s, is measured indirectly by measuring the cantilever response Δx_L. This local non-scanning approach has been applied to a thick PS film while ramping the temperature from 345 K to 395 K, Fig. 3. The response amplitude, Δx_L, in Fig. 3a shows a significant transition corresponding to the bulk T_g value of PS [19].

There are a few more advantages of the shear modulation technique over the friction force approach. The process can be easily automated with the MMR Technology temperature stage as described in the experimental section. A reliable statistical average is provided by the lock-in amplifier. Friction measurements are more difficult to average. A third advantage is the possibility of determining the phase relationship between the input disturbance and the response signal, Fig. 3b. The phase shift, or time delay of response, is a measure of the viscous properties of the material [41]. Note that the phase shift is not affected by the temperature. We will later come back to a more detailed discussion of the phase relationship and its connection with structural changes in the polymer matrix.

For now, we will address the generic shape of the amplitude response curve found in Fig. 3a, and compare it with bulk property measurements. As reviewed above, the shear modulus, G, is significantly altered when a polymer goes through T_g (a decay of up to three orders of magnitude). This however seems not to agree with the shear modulation measurements presented here. In Fig. 3a, there is a well-established lower plateau in the response amplitude, $\Delta x_L(T)$, below the glass transition, and the onset of a higher plateau above the glass transition is visible. Let us assume the shear modulation experiment could be pictured as two springs set in series with spring constants, k_s and k_L, representing the stiffness of the sample and the cantilever, respectively. The one-dimensional spring constant of the sample, k_s, is proportional to the shear modulus. Assuming fully elastic deformation during the shear process, Hooke's law applies, i.e.,

$$k_s \Delta x_s = k_L \Delta x_L = k^* (\Delta x_s + \Delta x_L);\ k^* = \left(\frac{1}{k_s} + \frac{1}{k_L} \right)^{-1} \tag{8}$$

where k^* is the overall spring constant of the system, and Δx_s is the sample deformation. As already established, the shear modulus is a function of the temperature, and hence, also $\Delta x_s(T)$. Let us further assume that $k^*(T_1) > k^*(T_2)$, and T_1 and T_2 represent temperatures below and above T_g, respectively. The experiment is conducted at a constant amplitude, Δx, and

$$\Delta x = \Delta x_s\,(T) + \Delta x_L\,(T). \tag{9}$$

As k_L is a constant and does not depend on T, it follows that $\Delta x_L(T_1) > \Delta x_L(T_2)$. This is, as already mentioned, in contradiction with the generic shape of the response curve in Fig. 3a.

In contact mechanics, the quality of the contact, i.e., the contact stiffness, k_s, is crucial, Eq. (8). The contact stiffness is responsible for the energy transport between cantilever and sample [41, 43]. The contact stiffness can be expressed for an adhesive elastic sphere-plane contact as [44, 45]

$$k_s = 8Ga;\ a^3 = \frac{3R}{4E}\left(L + 6\pi R\gamma + \sqrt{12\pi R\gamma L + (6\pi R\gamma)^2} \right) \tag{10}$$

with the contact radius, a, the radius of the spherical tip, R, the Young's and shear moduli of the sample, E and G, respectively, the externally applied load, L, and the interfacial energy per unit area, γ. To simplify the discussion, let us set L=0, which will not affect the following qualitative conclusions. We introduce the Poisson's ratio, ν, as

$$G = \frac{E}{2(1+\nu)} \tag{11}$$

Combining equation (10) and (11), the contact stiffness is rewritten as

$$k_s = 8\left(\frac{9}{2}\pi \frac{\gamma}{(1+\nu)} (RG(\omega))^2 \right)^{1/3} \tag{12}$$

where $G(\omega)$ represents the frequency dependent shear modulus. From Eq. (12), we can infer that the significant changes in the contact stiffness in Fig. 3a are due to changes in the interfacial interaction strength, the radius of curvature, and the Poisson's ratio. As discussed for our friction measurements, we have found that γ is significantly increasing at T_g. That alone would explain why we observe an increase in the response amplitude, Δx_L, i.e., an increase in the contact stiffness. Currently, these results are still only qualitative because of the difficulties in determining the contact area or the exact shape of the contact.

We also recorded the response amplitude while scanning. We did not find any strong effect due to the sliding motion (1 μm/s) or due to the occurring turning points

[46]. The reason why turning points did not affect our measurements is the fact that *stiction* was avoided with the constant shear motion. The advantages of mixing lateral disturbances into the scanning process is discussed elsewhere [42].

Interfacial confinement and surface T_g

Friction and adhesion measurements conducted on PS films as a function of the film thickness are presented in Figs 4a and b. As observed in previous studies on similar monodisperse amorphous polymer systems [3, 5, 6], we found that the friction force decreases below a critical thickness, t_{c1}, of about 100 to 150 nm, Fig. 4a, while the adhesion force is unaffected by the temperature change, Fig. 4b. The constant adhesion force indicates that the difference in friction is due to changes in the interfacial interaction or the shear modulus. As discussed above, a decrease in the interfacial interaction would go along with a decrease in friction. Based on the classical adhesive theory of Bowden and Tabor, the friction force can be related to the shear modulus by [41]

$$F_F = \tau_0 \pi \left(\frac{3RL}{4E} \right)^{2/3} + \alpha L \tag{13}$$

where $\tau=\tau_o+\alpha P$ is the shear strength and α is the correction coefficient which takes account of any pressure (P) dependence of the shear strength. Equation (13) indicates that a decrease in friction goes along with an increase in the elastic modulus. In other words, the PS film is constrained within a boundary regime of thickness t_{c1} towards the substrate surface.

Interfacial effects over such long distances are unexpected in a system that is well described as a Van der Waals liquid. Before we continue, and introduce very recently obtained surface glass transition data that is in good correspondence with the friction results above, we will briefly summarize previous findings concerning long-range interfacial confinement effects of spin-coated amorphous polymers. The conclusions presented here were drawn from extensive measurements obtained by various complementary techniques (SFM [3, 6], secondary ion mass spectrometry

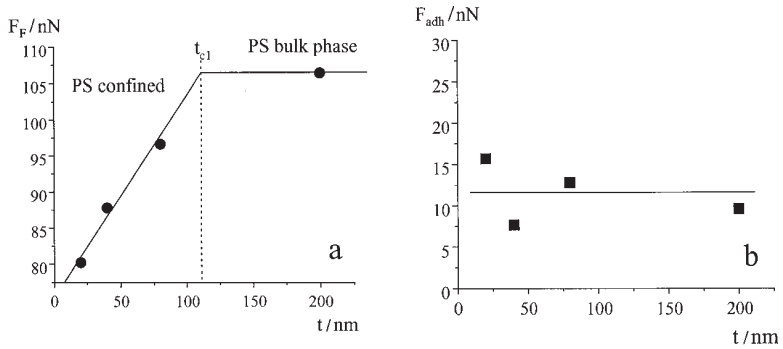

Fig. 4 Friction (a) and adhesion (b) *vs*. film thickness at room temperature. t_{c1} is a critical thickness below which friction decreases with film thickness

(SIMS) [3], neutron reflectivity [4, 47], and X-ray reflectivity [6]). It is believed that the structure of spin coated amorphous polymers is heterogeneous up to a distance of several hundreds of nanometers from the substrate surface. This heterogeneous layer is found to consist of two regimes: a gel-like sublayer at the interface (density loss of about 10% compared to the bulk polymer [6]), and an intermediate and gradually changing boundary layer (with a thickness of 7–10 R_g) [4, 6].

It is fairly easy to understand the change in mechanical properties and mobility for film thickness on the order of two times the radius of gyration (R_g), where almost every chain has at least one point of contact with the surface. On the other hand, the persistence of the effect at distances much larger than R_g, where most of the chains are not in direct contact with the surface, is far more difficult to explain. Existing classical mean field or molecular dynamic theories assume that the surface interaction is completely screened within a distance corresponding to the persistence length of the polymer (about 0.6 nm) [1, 2]. It was, however, found that this assumption is not valid in the case of spin-coated films where a layer immediately adjacent to the silicon substrate is pinned to the surface [4, 6]. Consequently, the large spin-coating-induced deformation of the chains cannot relax. The strained interfacial sublayer can be pictured as highly disentangled and laterally anisotropic, with a thickness on the order of R_g [6]. The polymers adjacent to the surface immobilized sublayer can diffuse through the sublayer's pores forming a two-fluid-system, as observed in diffusion measurements in a PS system [4]. At a distance of about 7–10 R_g apart from the substrate, the polymer behaves like the bulk elastomer and loses any memory of the presence of the silicon surface and the spin-coated induced interfacial alignment [4, 6].

In Fig. 5, the effect of the interfacial confinement on the surface glass transition temperature of PS is shown. The T_g value is steadily increasing with decreasing thickness in the ultrathin thickness regime between 20 and 110 nm. It is interesting to note that for films thinner than 20 nm no transition could be observed. This second critical

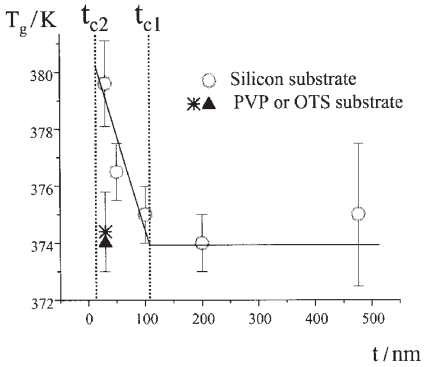

Fig. 5 Surface glass transition *vs*. film thickness. For films with a thickness between t_{c1} and t_{c2} (boundary regime) the glass transition is elevated. Below t_{c2} no glass transition is found (sublayer regime). T_g values were found to be independent of the PS film thickness for low interaction interfaces such as PVP and OTS

value corresponds to the radius of gyration of the polymer and the thickness of the gel-like sublayer [6]. An increase in T_g indicates that the material is mechanically confined, and that more thermal energy is necessary to induce a transition from a glass-like behavior to a melt. This is in excellent agreement with the friction results, Fig. 4a, discussed above.

We have reviewed that the confinement effect is due to the spin coating process and the presence of an interfacially interactive substrate. It has been found, that films remain strained even after several temperature annealing attempts [6]. Thus, one would expect that if the PS film was transferred to a low interaction surface and annealed, the strain would disappear. We chose thin films of PVP and OTS as low interaction interfaces, which were 'sandwiched' between the silicon substrate and PS films. As expected, a transition temperature value corresponding to the bulk glass transition temperature was found at the surface for all PS films even the ones far thinner than the critical thickness of $t_{c1} \cong 110$ nm, Fig. 5.

The possibility of solid substrate sampling and the effect of load

We have been very careful in analyzing our friction measurements and shear modulation measurements in regards of their qualitative behavior. In all of our considerations so far, it was implicitly assumed that measurements have been obtained at the surface of the polymer. Not neglected was the possibility that the tip sinks (or creeps) into the polymer matrix after the temperature reaches or exceeds the glass transition temperature. From adhesion force measurements, we conclude that changes in the contact area, which would be expected if we sink in, are small at $T<T_g$. Further, we transferred PS films of various thicknesses on low interaction interfaces such as PVP and OTS and found the bulk T_g confirmed even at films as thin as 20 nm. That is the strongest indication that we do not sample the substrate either indirectly or by sinking in and breaking through before T_g is reached. Finally, we performed repeated shear modulation measurements to document reproducibility (Fig.6).

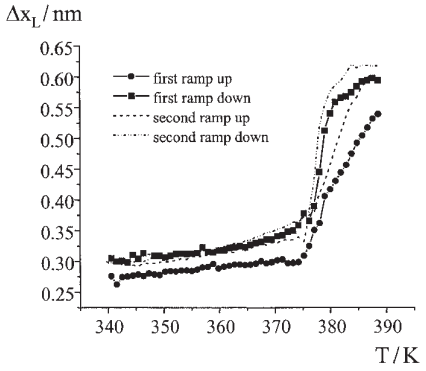

Fig. 6 Repeated shear modulation measurements at the same location show high reproducibility

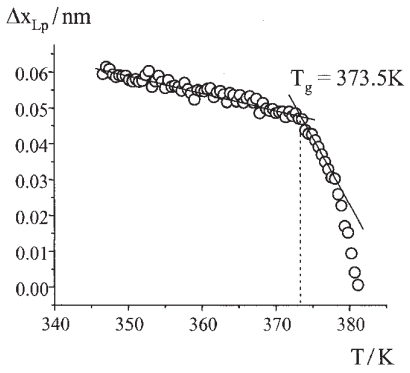

Fig. 7 The qualitative behavior of the shear modulation response amplitude, Δx_L, decreases above T_g for low loads. The transition value obtained on a 200 nm thick PS film is unaffected, i.e., still corresponds to the bulk glass transition temperature

No significant loading effects on the critical transition temperature were found in shear modulation measurements. The qualitative behavior of the response amplitude with temperature was however affected by the load, Fig. 7. At a very low load of 5.4 nN the cantilever and the sample lost contact in the course of the heating process above the glass transition temperature. The process of loosing contact significantly influenced the contact stiffness, which is found to decrease with increasing temperature above T_g. This process can be understood in terms of dewetting or energy minimization. Polymers have a low interaction energy and close to negative spreading coefficient with silicon oxide. Given time and sufficient mobility the polymer will try to minimize the contact with the silicon tip. Thus, heating the polymer-silicon interface above T_g at very low load will cause dewetting.

Structural phase transitions

The glass transition of amorphous polymers, as reviewed above, is well described by the free volume theory that treats the transition as an isotropic expansion where free volume is formed. The free volume provides the polymers with some dynamic degrees of freedom. The theory does not address bulk structural recombinations that would affect the surface energy.

The data, retrieved from contact mechanical measurements, contains information about the interface and the bulk. To improve our understanding and to support some previous statements on how nano-contact shear modulation measurements are affected by structural changes, we chose a polymer that is well known for its structural phase transition. The sample of choice is *N*-isopropylacrylamide (NIPAM), and the environment is water. NIPAM undergoes a structural phase transition at a lower critical solution temperature, T_c, of 302 K [49]. Below T_c the polymer has a highly hydrated gel-like structural conformation, while above T_c the gel collapses and deswells.

The structural phase transition of NIPAM is fully reversible driven by hydrophobic forces and hydrogen bonding. Below T_c, i.e, in the gel-like phase, the polymer segments are stretched beyond their equilibrium length, and the hydrogen bonds and water prevent the collapse of the gel. By increasing the temperature this force balance is disturbed as the polymer segmental kinetics increases. At T_c, the elastic compression forces exceed the hydrogen bonding forces. With diminishing hydrogen bonding interaction sites the water is expelled from the gel, and the gel structure collapses. This structural phase transition is accompanied by a change in the volume and a dramatic change in the mechanical properties [49]. In literature the behavior of NIPAM is well described by the Flory theory for non-ionic gels [50]. The Young's modulus of NIPAM has been determined with Flory's theory by volume change experiments and was found to be $9.8 \cdot 10^3$ Pa at 25ºC and $1.7 \cdot 10^5$ Pa at 40ºC [51]. Observations of Young's and shear moduli suggest that the Poisson's ratio is not constant and is significantly decreasing at T_c [52, 53].

We applied the shear modulation method in an aqueous environment to a CVD film of NIPAM and found a transition temperature of 301.5 K, which corresponds to the bulk structural phase transition temperature T_c, Fig. 8 [35].

As elucidated above, shear modulation experiments with the SFM are sensitive to changes in the shear modulus, G, the interfacial interaction strength, γ, and the Poisson's ratio, ν. Our observations regarding changes in the shear amplitude response are interpreted based on the reported information of bulk NIPAM and adhesion force measurements. In adhesion force measurements, we estimated the strength of the contact between tip and sample below and above T_c. We found that the interaction between the silicon oxide tip and the NIPAM sample is slightly repulsive below T_c and attractive above T_c. Thus the structural change is strongly influencing the interfacial interaction. Considering Eq. (12), Fig. 8 is in qualitative agreement with that finding. The reported increase in the bulk moduli, due to structural changes from a temperature below to temperature above T_c, is apparently also in agreement with the change in the shear response amplitude. However, due to high modulation frequency, the shear response amplitude is more sensitive to the interfacial interaction strength than to the shear modulus.

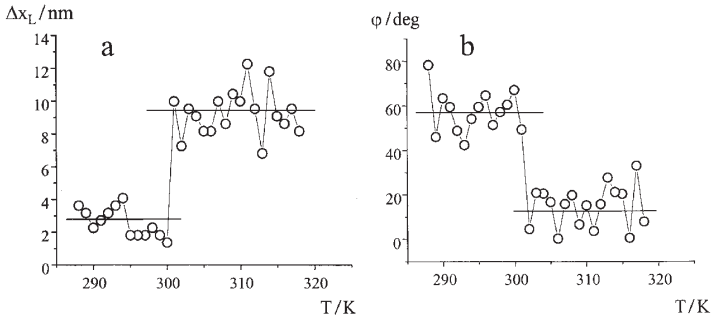

Fig. 8 Shear modulation amplitude, Δx_L, and phase responses, φ, *vs*. temperature on poly-NIPAM. A transition of 301.5 K is found that corresponds to the bulk structural phase transition temperature, T_c

Both, the shear amplitude response and the phase shift show a very pronounced transition. While we have not found a functional relationship between the phase shift and temperature on PS, we observed a 50 degrees phase lag on NIPAM, Fig. 8b. As stated previously, there is a significant difference between the two transitions. T_g is indicating an almost structurally isotropic transition while T_c is denoting a structural transition. Thus, the phase shift measurements are sensitive to the magnitude in structural changes, which affect the viscous properties. From Fig. 8, it is deduced that the viscosity of the system decreases with the collapse of the gel [35].

In summary, we find that the NIPAM measurements confirm our previously stated conclusion that at high frequency measurements the amplitude and phase of the shear modulation response are measures of the sample's surface energy and the near surface viscous property, respectively [35].

Summary and outlook

This paper reviewed our recent research efforts in employing nano-contact mechanics to determine the surface glass transition temperature of amorphous polymer films such as PS and PtBA.

We investigated the free surface of thick bulk-like films and found that for polymers with molecular weights larger than 30*k* the surface glass transition corresponds to the glass transition of the bulk polymer. For ultrathin films, i.e, film thicknesses on the order of 200 nm or less, confining effects due to the close substrate and the film preparation technique can significantly alter the phase of the polymer. We found that the PS phase is constrained within a boundary layer of about 110–150 nm towards the silicon substrate. This interfacial long-range confinement effect, as it was found in previous studies, is due to the occurrence of increased lateral disentanglement of polymer chains during the spin coating process, and the interactive interface that does not permit temperature annealing. The heterogeneous structure that is established normal to the substrate surface is creating phase or property gradients in the PS matrix. For films thinner than 150 nm, the glass transition temperature increases the closer the film is measured from the substrate surface. At a distance of around 20 nm, a transition is no longer observable.

We introduced two modes of operation to determine the surface glass transition temperature; the scanning friction mode and the locally-fixed shear modulation mode. The information contained in the friction force signal was deconvoluted and addressed to the contact area and the interfacial interaction strength by employing friction-load and adhesion force measurements. Shear modulation mode measurements with frequencies above the inertia of the PS melt were found to be sensitive to changes in the interfacial interaction. Interfacial interactions are dependent on the surface energy that is strongly related to the structural conformation. With NIPAM measurements, we illustrated the sensitivity of the shear modulation response amplitude to changes in the surface interaction. In that regard, the nano-contact mechanical approach is comparable to dielectric and refractive index measurements; i.e., properties that are responsible for interfacial interactions (see Hamaker constant). As a third

SFM contact mechanical mode, phase shift measurements were introduced. The phase shift, known to be a measure of the material's viscous properties [54], was found to be a measure of the subsurface structural conformation. It was found as expected that NIPAM compared to PS experienced a much larger structural change when going through the thermally activated transition.

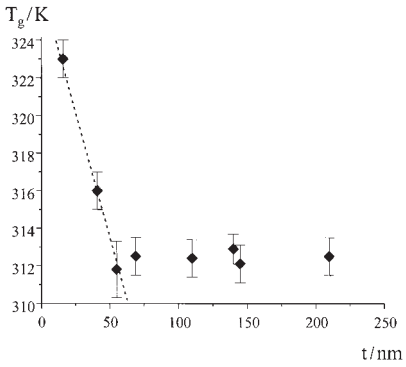

Fig. 9 Surface glass transition *vs*. film thickness of PBMA. Above 50 nm, the transition temperature corresponds to DSC bulk measurements (314 K)

The outlook of such nano-mechanical approaches to determine the surface glass transition temperature, as illustrated, is manifold. The findings presented above are not isolated. On the contrary, we found interfacial confining effects for many more polymer systems that were spin coated (for instance, for poly *n*-butyl methacrylate, Fig. 9). We expect from such nanocontact mechanical approaches to learn more about macroscopic properties of complex polymeric systems, which contain a multiple of interfaces and constraints. Future experiments will involve binary and multi-component systems were confinement occurs multidimensionally.

* * *

This work was supported by the Shell Foundation's Faculty Career Initiation Fund, and the NSF MRSEC (DMR96324235). Acknowledgment is made to the Donors of The Petroleum Research Fund, administered by the American Chemical Society, for partial support of this research. Reto Luginbühl was supported by the University of Washington Engineered Biomaterials (UWEB) program, a NSF ERC (EEC 9529161). The authors of this review paper would like to thank Robert Paugh from MMR Technology Inc. for instrumental support, and Miriam Rafailovich, Jonathan Sokolov, and Shouren Ge from the State University of New York at Stony Brook for taking part on the initiation of this research.

References

1 P. G. de Gennes, Scaling Concepts in Polymer Physics, Cornell Univ. Press, Ithaca, NY, 1979.
2 M. Brogley, S. Bistac and J. Schultz, Macromol. Theor. Simul., 7 (1998) 65.

3 R. M. Overney, L. Guo, H. Totsuka, M. H. Rafailovich, J. Sokolov and S. A. Schwarz, Mat. Res. Soc. Symp. Proc., 464 (1997) 133.
4 X. Zheng, M. H. Rafailovich, J. Sokolov, Y. Strzhemechny, S. A. Schwarz, B. B. Sauer and M. Rubinstein, Phys. Rev. Lett., 79 (1997) 241.
5 R. M. Overney, D. P. Leta, L. J. Fetters, Y. Liu, M. H. Rafailovich and J. Sokolov, J. Vac. Sci. Technol., B 14 (1996) 1276.
6 C. Buenviaje, S. Ge, M. Rafailovich, J. Sokolov, J. M. Drake and R. M. Overney, Langmuir, 15 (1999) 3521.
7 T. Kajiyama, K. Tanaka and A. Takahara, Macromolecules, 2 (1997) 280.
8 Y. Liu, T. P. Russell, M. G. Samant, J. Stohr, H. R. Brown, A. Cossy-Favre and J. Diaz, Macromolecules, 30 (1997) 7768.
9 X. Zheng, B. B. Sauer, J. G. Van Alsten, S. A. Schwarz, M. H. Rafailovich, J. Sokolov and M. Rubinstein, Phys. Rev. Lett., 74 (1995) 407.
10 B. Frank, A. P. Gast, T. P. Russel, H. R. Brown and C. Hawker, Macromolecules, 29 (1996) 6531.
11 J. H. Van Zanten, W. E. Wallace and W. L. Wu, Phys. Rev. B, 53 (1996) R2053.
12 W. E. Wallace, J. H. van Zanten and W. L. Wu, Phys. Rev. B, 52 (1995) R3329.
13 I. Entin, R. Goffer, D. Davidov and I. Hersht, Phys. Rev. B, 47 (1993) 8265.
14 J. C. Jean, R. Zhang, H. Cao, J.-P. Yuan, C.-M. Huang, B. Nielsen and C.-M. Huang, Phys. Rev. B, 56 (1997) R8459.
15 G. B. DeMaggio, W. E. Frieze, D. W. Gidley, M. Zhu, H. A. Hristov and A. F. Yee, Phys. Rev. Lett., 78 (1997) 1524.
16 J. L. Keddie, A. L. Jones and R. A. Cory, Europhys. Lett., 27 (1994) 59.
17 J. A. Forrest, K. Dalnoski-Veress, J. R. Stevens and J. R. Dutcher, Phys. Rev. Lett., 77 (1996) 2002.
18 O. Prucker, S. Christian, H. Bock, J. Ruehe, C. Frank and W. Knoll, Macromolecular Chemistry and Physics, 199 (1998) 1435.
19 R. M. Overney, Langmuir, to be submitted for publication.
20 C. Buenviaje, F. Dinelli and R. M. Overney, to appear in ACS Symp. Series, 'Interfacial Properties on the Submicron Scale', eds. J. Frommer and R. Overney, Oxford Univ. Press, Oxford.
21 T. Kajiyama, K. Tanaka and A. Takahara, Polymer, 39 (1998) 4665.
22 J. A. Hammerschmidt, W. L. Gladfelder and G. Haugstad, Macromolecules, 32 (1999) 3360.
23 S. C. Kuebler, A. Heuer and H. W. Spiess, Phys. Rev., E 56 (1997) 741.
24 A. Eisenberg, in J. E. M. et al. (Ed.): Physical Properties of Polymers, 2nd edition, ACS, Washington DC 1993.
25 T. G. Fox and P. J. Flory, J. Appl. Phys., 21 (1950) 581.
26 E. M. Frith and R. F. Tuckett. Linear Polymers, Longmans, Green, London 1951.
27 M. L. Williams, R. F. Landel and J. D. Ferry, J. Am. Chem. Soc., 77 (1955) 3701.
28 A. D. Jenkins, Polymer Science, Vol. 1, North Holland Publ. Company, Amsterdam 1972.
29 A. K. Doolittle, J. Appl. Phys., 22 (1951) 1471.
30 J. M. O'Reilly and M. Goldstein, Structure and Mobility in Molecular and Atomic Glasses, New York Academy of Sciences, New York 1981.
31 F. H. Stillinger, J. Chem. Phys., 88 (1988) 7818.
32 Y. V. Pan, M. Mar, M. M. Takeno, B. D. Ratner and D. D. Denton, Applications of plasma polymer films as non-fouling and thermally responsive coatings in biomaterials and MEMS. Materials Research Society Fall Meeting (Boston) 1998.

33 R. Luginbühl, M. D. Garrison, R. M. Overney, L. Weiss, H. Schiefendecker, S. Hild and B. D. Ratner, to appear in ACS Symp. Series, eds. D. Castner and D. Grainger, Oxford Univ. Press, Oxford.
34 P. Favia, V. H. Perez-Luna, T. Boland, D. G. Castner and B. D. Ratner, Plasmas and Polymers, 1 (1996) 299.
35 R. Luginbühl, Y. V. Pan, B. D. Ratner and R. M. Overney, to be submitted for publication.
36 C. Buenviaje, S. Ge, M. H. Rafailovich and R. M. Overney, Mat. Res. Soc. Symp. Proc., 522 (1998) 187.
37 R. Overney and E. Meyer, Mat. Res. Soc., 18 (1993) 26.
38 R. M. Overney, TRIP, 3 (1995) 359.
39 D. H. Gracias, D. Zhang, Y. R. Shen and G. A. Somorjai, Mat. Res. Soc. Symp. Proc., 522 (1998) 175.
40 F. Dinelli, C. K. Buenviaje and R. M. Overney, submitted to J. Chem. Phys.
41 E. Meyer, R. M. Overney, K. Dransfeld and T. Gyalog, Nanoscience: Friction and Rheology on the Nanometer Scale, World Scientific Publ., Singapore 1998.
42 R. Luginbühl and R. M. Overney, to be submitted for publication.
43 R. W. Carpick, D. F. Ogletree and M. Salmeron, Appl. Phys. Lett., 70 (1997) 1548.
44 K. L. Johnson, K. Kendall and A. D. Roberts, Proc. Royal Soc., A 324 (1971) 301.
45 K. L. Johnson, Contact Mechanics, Cambridge University Press, Cambridge, 1985.
46 R. Luginbühl, M. D. Garrison, R. M. Overney and B. D. Ratner, submitted (1999).
47 W. E. Wallace, N. C. B. Tan and W. L. Wu, J. Chem. Phys., 108 (1998) 3798.
48 B. R. Saunders and B. Vincent, Advances in Colloid and Interface Science, 80 (1999) 1.
49 A. Suzuki and S. Kojima, Journal of Chemical Physics, 101 (1994) 10003.
50 P. J. Flory, Principles of polymer chemistry, Cornell University, Ithaca, NY, 1966.
51 Y. Suzuki, K. Tomonaga, M. Kumazaki and I. Nishio, Polymer Gels and Networks, 4 (1996) 129.
52 C. Li, Z. Hu and Y. Li, Physical Review E (Statistical Physics, Plasmas, Fluids, and Related Interdisciplinary Topics), 48 (1993) 603.
53 S. Hirotsu, Journal of Chemical Physics, 94 (1991) 3949.
54 R. M. Overney, D. P. Leta, C. F. Pictroski, M. H. Rafailovich, Y. Liu, J. Quinn, J. Sokolov, A. Eisenberg and G. Overney, Phys. Rev. Lett., 76 (1996) 1272.